Analysis of the Hall D Tagger Dipole Magnet Field Maps

Daniel I. Sober
The Catholic University of America
2 July 2015

1. Introduction

The photon tagging system for Hall D is essential for defining the incident photon energy of the GlueX experiment, and also for the alignment of the diamond crystal radiator in order to place the desired coherent peak at the correct photon energy. The photon energy is determined by precise measurement of the energy of the bremsstrahlung electrons by their deflection in the field of the tagger dipole magnet. The energy calibration of the system thus requires precise knowledge of this magnetic field.

2. Goals

The intended energy resolution of the GlueX experiment requires a goal of approximately 12 MeV (or 0.1% of the incident election energy) in the tagged photon energy. The tagged photon energy is determined by the energy calibration of the tagging system, both for the bremsstrahlung electrons which are detected on the focal plane and for the full-energy electrons which travel to the electron beam dump (which determines the magnetic field setting for the tagger magnet.) Consistency with this goal requires that the magnetic field integrals along all useful electron trajectories be known to about 0.1%.

Since the deflection of the electron trajectory depends on both the magnetic field value and its boundaries, the accuracy of the magnetic field measurements should satisfy the following goals :

- Better than 0.1% accuracy in average field (15 gauss at 1.5 T)
- ~3 mm accuracy in the absolute positions of the magnet entry and full-energy exit edges
- ~0.5 mm accuracy in the absolute position of the long exit edge

In this note, it is shown that the magnetic field maps measured by the JLab engineering group in January-February 2014, augmented by detailed Tosca calculations performed earlier by Guangliang Yang at Glasgow University, allowed us to meet these goals.

3. Field mapping measurements

The field mapping was performed by Tim Whitlatch et al., between 07 January and 11 February 2014, using a specially constructed translation system and an array of five Hall probes which measured the vertical (Z) component of the field at five positions. Figure 1 shows a sketch of the tagger magnet and the mapping coordinate system. The magnet Y-axis is inclined at 6.5° to the incident beam axis.

The five probes were separated by 1 cm in the X-direction. At each X position, the probe carriage was stepped in Y, and five X-values were measured simultaneously. After each Y sweep, the carriage was advanced by 4 cm in X (so that Probe 1 repeats the point measured by Probe 5 on the previous sweep.) The mapping apparatus was not large enough to measure the

entire required region (~65 by 650 cm) in a single setting, so it was necessary to move and realign the mapper apparatus several times. In all, there were 6 configurations, as shown in Figure 1 and described in Table I.

Configurations 1 and 3 covered the uniform-field region with a grid of 1 cm in X and 2.5 cm in Y. Configurations 2 and 4 covered the fringe region outside the long exit edge with the same grid spacing. Configuration 5 covered the full-energy exit region with a 1 cm by 1 cm grid. Configuration 6 was a special setup which used a single probe to measure the field in 1-cm steps along the axis of the incident electron beam. Each configuration had some overlap with its neighboring regions to allow checks of consistency.

For each configuration, the field was measured at 3 settings:

1.7 Tesla (corresponding to 13.6 GeV)
1.5 Tesla (12 GeV)
0.75 Tesla (6 GeV)

Since the Tosca calculations predicted that the variations in field shape with excitation would be very small over this range (of order 0.1% or less), it was concluded that these three values would be sufficient for interpolation to any possible beam energy. When not otherwise stated in this document, the 1.5 T map (12 GeV) is always assumed.

Table I shows the properties of the six mapped configurations.

4. Probe calibrations

Before the first configuration was measured, and three other times during the mapping, the five probes were calibrated by inserting them to a fixed position inside the uniform field region and comparing them to an NMR probe. This calibration was performed at the three excitations corresponding to the measured maps. Figure 2 shows the calibration ratios. (Note: I have renumbered the probes B1-B5 so that the X coordinate always increases with probe number. The original numbering of Probes 1-5 by the mapping group was opposite to this for Configurations 1 and 2, and then reversed, so each plot except B3 includes a change of hardware.)

While in principle there should be no difference between the Hall/NMR ratios at the three excitations, the actual ratios at each calibration date varied by up to 0.05%. To allow for possible nonlinearity in the Hall probe, it was decided to use the calibration ratio for each field setting in analyzing the maps at that field. In addition, the calibration ratios varied with time, in some cases by up to 0.1% between measurements. It was decided to use the calibration ratios measured closest in time to the mapping for each configuration.

A few corrections to the probe calibrations were necessary. In particular, Probe B2 began to show a substantial drift during the measurement of Configuration 1, so empirical calibration values (based on comparison of neighboring field values) were used for Configuration 2. This probe was replaced by a new probe for Configurations 3-6.

The measured probe calibrations ("Calibration 1") were adequate to give a field uniformity of order 0.05% (8 gauss at 1.5 T) in the uniform field region, but some variation with a period of 4 cm in X (the distance between successive positions of the mapping carriage) was clearly apparent in the data. These ripples had no serious effect on the ray-tracing, but gave a somewhat misleading appearance to the field contour plots, so at a later date (January-February 2015) I used data ratios to recalibrate the probes for the uniform-field region (Configurations 1 and 3). The recalibration had only a small effect on the energy calculations: the full-energy deflection changed by less than 0.0013%, and the energy at the focal plane changed by between 0 and -0.6 MeV (-0.1 to -0.2 MeV in the Microscope region, 3-4 GeV). I have decided to use the recalibrated probe constants ("Calibration 3") for all subsequent work on Configurations 1, 3 and 4. (Configuration 4 uses the same calibration set as Configuration 3.) The recalibrated probe constants are shown by the unfilled symbols in Figure 2.

Examples of the field uniformity before and after recalibration are shown in Figures 4-7.

5. Field properties and comparison with Tosca calculations

In my February 2014 presentation to the Collaboration (Field_mapping.pdf : Analysis of tagger magnet field maps, created 2/20/14; GlueX DocID 2411) I showed that

1) The field maps are mutually consistent in regions where the configurations overlap.

2) The field in the central region is somewhat less uniform than predicted by Tosca (with fractional differences of up to ±0.15%) but it is nearly symmetric with respect to Y, indicating that the effect is real and not an artifact of the mapping. At the two higher field settings, there is a slight increase of the field with X, which can be explained by a slight tilting of the poles due to magnetic forces.

2) The shape of the fringe field is in excellent agreement with Tosca calculations (so that Tosca can be used to extrapolate into unmeasured regions.)

3) The alignment of the mapping apparatus was excellent for the important dimensions (X along the long exit edge, Y at the entry and full-energy exit edges). There were alignment errors of up to several mm in some of the non-critical coordinates, but most of these had negligible effect on the raytracing, as discussed below.

6. Field analysis procedure

Table II summarizes the procedures used in analyzing the mapping data.

a. Data checking

First, the field values measured in each configuration were multiplied by the probe calibration factors and plotted as a function of X and of Y, to look for missing or anomalous points. In a few cases (as noted in the Table) some corrections were made by hand. Then an output map file (of B versus X and Y) was written for that configuration.

b. Alignment

At this point, the alignment of the field boundaries was checked carefully for each configuration. The shape of the field was described extremely well by the Tosca calculations, so it was possible to determine an alignment error by comparison with the scaled Tosca field. In a few cases (see Table III) the alignment was off by up to several millimeters, but in most cases this error could be ignored. For Configurations 1-4, the Y alignment was unimportant, because the variation was small except near the entry and full-energy exit edges, and the field in these regions was measured independently in Configurations 6 and 5 respectively. For Configurations 1 and 3, the X alignment was unimportant, because it affected the field only at $X < -13$ cm (where no electron trajectories passed) and at $X > 12$ cm, which was measured in Configurations 2 and 4.

The most sensitive boundary is at the long exit edge of the magnet, since the outgoing electrons cross this boundary at a grazing angle (11-12 degrees in the Microscope region, down to 8° for the highest-energy electrons.) The alignment of the mapping apparatus for Configurations 2 and 4, which include this edge, was at the level of better than ± 0.5 mm, but because of the rapid change of the field in the fringe region there was a significant difference (up to $\approx 2\%$) between the field values of Configurations 2 and 4 in their overlap region, which could be explained by a relative shift of 0.6 mm in the X coordinate. Furthermore, a careful analysis showed a small Y-dependence of the edge position, which possibly resulted from some curvature of the long beam of the mapping apparatus. Because of the sensitivity of this boundary, it was decided to adjust the field at each Y value so as to align the X boundary (defined as the X value where the field is half its maximum value at that Y value) with the Tosca boundary, using a cubic spline interpolation. This procedure, applied to the 1.5 T map, gave residual variations in the edge position of less than 0.01 mm. The same X shifts were applied to the 1.7 T and 0.75 T maps. The residual variations were less than 0.2 mm, so no further adjustment was deemed necessary.

c. Field boxes for raytracing

It was not possible to combine the full set of measurements into a single field box, because a finer spacing in X was required near the ends of the magnet, and a finer spacing in Y near the long exit edge. Thus Configurations 5 and 6 were measured on different grids from Configurations 1-4, and four different field boxes, named “Main”, “Entry”, “Exit” and “Focal”, were constructed for each excitation. Their properties are summarized in Table IV.

Configurations 1-4 contain the entire uniform-field region, as well as the measured fringe field outside the long magnet edge. These four configurations were merged into the “Main” field box, using the average field wherever multiple measurements were taken at the same X,Y value. (Because the X alignment of Configurations 1 and 3 was questionable, the points at the largest X, 12.5 cm, were not used.) The grid for the Main field box is 1 cm (in X) by 2.5 cm (in Y)

In the entry region, the field was measured only in 1-cm steps along the beam line (Configuration 6), extending into the uniform-field region of Configuration 1. In order to create a two-dimensional "Entry" field box in this region, the 1 cm by 1 cm Tosca field was scaled to the Configuration 6 data at each Y value. It was then checked that these values are consistent with Configuration 1 in the uniform region.

In the full-energy exit region, the data of Configuration 5 (taken on a 1 by 1 cm grid) were carefully checked for alignment and for consistency with the uniform region of Configuration 3. The resulting "Exit" field box had to be augmented by some scaled points from the Tosca field map in order to fully cover the full-energy exit ray region and to provide additional fringe field for the high-energy bremsstrahlung electrons.

Configurations 3 and 4 extend to X = 51.5 cm, where the field is of order 50 gauss. While the residual deflection in the remaining field before arriving at the focal plane is small, it is not completely negligible, so it was decided to create an additional "Focal" field box in which the electrons are transported further into the fringe field (down to 19 gauss or less) and closer to the focal plane. The field in this box was calculated using the Tosca field normalized to the average field in the uniform region of Configuration 5. Omitting the Focal box in the raytracing would lead to an energy error of 0.8 to 1.0 MeV in the Microscope region (3-4 GeV), with maximum error 1.4 MeV at 6 GeV.

The properties of the field boxes are summarized in Table IV. More details, including the specific format of the SNAKE input files, are given in the document "Hall D Tagger Dipole Field Maps" of 21 July 2014. Figure 3 shows the dimensions of the field boxes, some electron trajectories to the focal plane, and fringe field values at the boundaries.

Figures 4 and 5 show the X- and Y-dependence of the 1.5 T field in the Main box, both before and after the probe recalibration. Figures 6 and 7 show contour plots of the field in the Main box at all three excitations, before and after the probe recalibration.

7. Raytracing and energy calculations

a. Procedure

The program SNAKE was used to perform raytracing through the field boxes. At the present time, the quadrupole magnet has not been included in any calculations, and is assumed to be properly zeroed. The bremsstrahlung electron begins at the radiator in a field-free space (the "Target" box), then propagates into the Entry box where the raytracing begins. In each box, the particle is propagated forward in the field of that box until it crosses an "endplane", at which point the field definition is switched to the next overlapping box. After reaching the final endplane of the last box, the particle propagates in zero field to the focal plane. The endplanes are shown as heavy black lines in Figure 3.

Before beginning raytracing of the bremsstrahlung electrons, it is necessary to find the correct

scale factor for the magnetic field such that the full-energy electrons are deflected by exactly 13.4° for the nominal map energies of 13.6, 12.0 and 6.0 GeV. The angle is calculated at the endplane of the Exit box, where the fringe field is approximately 9 gauss. This scale factor is then applied to all the field boxes for subsequent raytracing at that energy. The scale factors are shown in Table V.

The coverage of the field boxes requires that different raytracing procedures be used for low-energy and high-energy electrons. For E_0 = 12 GeV,

$E \leq 6.99$ GeV: raytrace through Entry + Main + Focal boxes

$E \geq 6.67$ GeV: raytrace through Entry + Main + Exit boxes

Different endplanes in the Main box are used in the two cases. For $6.67 \leq E \leq 6.99$ GeV, the calculations can be done either way and give essentially identical results (differing by less than 0.06 mm along the focal plane.)

b. Energy and derivatives

For on-axis trajectories from the radiator, the electron energy is related uniquely to the local "x_{FP}" coordinate along the focal plane. For most purposes, the energy boundaries of the detector channels are adequately described by these on-axis rays. To determine the magnet optics in more detail, it is necessary to generate electron trajectories with non-zero x and z positions and angles at the radiator. For a first attempt, I generated trajectories from a point source at the radiator with steps of 30 MeV in energy and displacements of 0, $\pm\theta_{ce}$ and $\pm 2\theta_{ce}$ in horizontal and vertical angle, where θ_{ce} is the electron characteristic angle for a bremsstrahlung electron of energy E, $\theta_{ce} \equiv (m/E_0)\,(E_0 - E)/E$. The results show that the effects of the angular displacements are very nearly linear, so that a set of first derivatives should be sufficient. Next, I generated trajectories (at E_0 = 12 GeV, 30 MeV steps) with initial displacements of 0 and +1 mm in x and z, and 0 and +1 θ_{ce} in the x and z angles. These rays are then propagated through the magnet to the focal plane, and the results are used to make tables of E, x_{FP}, θ_X and derivatives (of final x, z, θ_X and θ_Z with respect to initial x, z, θ_X and θ_Z) which can be used to calculate the trajectory at any counter position.

Files of positions, angles and derivatives versus electron energy were posted on the GlueX Wiki in June and July 2014. A new set of tables using the map with recalibrated probe constants was constructed in June-July 2015.

c. E_0-independence of results

An important result of the raytracing studies is that the energy calibration at the focal plane is essentially constant as a function of E/E_0 for all three field maps. Using the 1.5 T (12 GeV) map and scaling the field to the appropriate E_0 will give an energy error of less than 3.4 MeV anywhere on the focal plane for E_0 = 13.6 GeV (less than 2.0 MeV in the Microscope region), and less than 0.8 MeV (0.2 MeV) at E_0 = 6.0 GeV. Figure 8 and Table VI summarize the consistency of the three field maps in energy reconstruction. Given this result, it is probably unnecessary to use the 0.75 T and 1.7 T field maps at all, although we could not have known this if we had not measured and analyzed them.

For the (unlikely) event that anyone wishes to improve the accuracy of the energy and angle reconstruction by interpolating between the results calculated from two field maps, I have derived some interpolation algorithms based on the Tosca calculations at intermediate field values (0.9, 1.2, 1.4, and 1.6 Tesla). They are explained in a separate note, "Interpolation between the Hall D tagger dipole field maps."

References

The following documents are available on the GlueX Wiki, and give more detailed information about some of the topics covered in this note.

Field_mapping.pdf	20 Feb 2014	Analysis of tagger magnet field maps (presentation to collaboration meeting)
Field_boxes_and_headers.pdf	21 July 2014	Hall D tagger dipole field maps (format of files)
E0_interpolation.pdf	1 July 2015	Interpolation between the Hall D tagger dipole field maps

Tables and Figures

Table I Summary of measured field maps. The field was set to 7500, 15000 or 17000 gauss using the NMR probe at a fixed reference position. The NMR values recorded in the data files differed slightly from the nominal values due to small drifts or reading errors. The nominal values were assumed for the analysis.

Configuration	Y [cm]	X [cm]	NMR [g]	Dates
1	-306.35 to 13.65 by 2.5	-14.5 to 13.5 by 1.0	7501 15001 17000	1/9/14 1/8/14 1/7/14
2	-276.35 to 13.65 by 2.5	11.5 to 51.5 by 1.0	7500 15001 16999	1/15/14 1/15/14 1/14/14
3	-16.35 to 308.65 by 2.5	-14.5 to 13.5 by 1.0	7498 14999 17001	2/4/14 2/3/14 2/4/14
4	-3.65 to 308.65 by 2.5	11.5 to 51.5 by 1.0	7497 15002 ~17000	2/7/14 2/6/14 2/6/14
5	293.65 to 334.65 by 1.0	7.5 to 51.5 by 1.0	7499 14999 16999	2/11/14 2/11/14 2/10/14
6	-346.35 to -296.35 by 1.0	9.90 to 3.85 along beam line	7501 15001 17001	1/21 1/21 1/21

Table II. Summary of field map analysis procedure.

Configuration	Boundaries (cm)	Procedure	Output files
1 (upstream, uniform)	*x*: -14.5 to 13.5* by 1.0 cm step *y*: -308.85** to 13.65 by 2.5 cm step **x*=13.5 omitted from merge because of alignment error **1.5T map begins at *y*=−306.35	Probe calibration data: 1/06/14. 1.7T: fix 1 data point 0.75T: fix 1 data point *x* is misaligned by ≈7 mm, but not significant if *x*=13.5 point omitted from merge	1.5c1.map merged into main15.map 0.75c1.map merged into main75.map,... (see below for limits)
2 (upstream, fringe)	*x*: 11.5 to 51.5* by 1.0 cm step *y*: -276.35* to 13.65 by 2.5 cm step * absent triangular corner from (*x*,*y*) = (28.5, -276.35) to (51.5, -263.85)	Probe calibration data: 1/16/14 with modifications for ailing Probe B2. 1.5T: fix 3 data points 1.7T: fix 18 data points For each *y*, adjust *x* to align half-field points with Tosca.	1.5c2.map merged into main15.map: *y*: -306.35 to 308.65 by 2.5 *x*: -14.5 to 51.5 by 1.0 ...
3 (downstream, uniform)	*x*: -14.5 to 13.5* by 1.0 cm step *y*: -16.35 to 308.65 by 2.5 cm step **x*=13.5 omitted from merge	Probe calibration data: 1/31/14	1.5c3.map merged into main15.map ...
4 (downstream, fringe)	*x*: 11.5 to 51.5 by 1.0 cm step *y*: -3.85 to 308.65 by 2.5 cm step	Probe calibration data: 1/31/14 For each *y*, adjust *x* to align half-field points with Tosca.	1.5c4.map merged into main15.map ...
5 (full-energy exit)	*x*: 7.5* to 15.5* by 1.0 cm step *y*: 293.65* to 334.65 by 1.0 cm step * absent rectangular corner from (*x*,*y*) = (7.5, 297.65) to (10.5, 293.65)	Probe calibration data: 2/12/14 No realignment required. Create field box on measured grid, with missing points calculated using scaled Tosca field.	exit15.map, exit75.map, ... *x*: 0.5 to 70.5 by 1.0 *y*: 293.65 to 360.65 by 1.0
6 (entry)	*x*: 3.854 to 9.904 (single line) *y*: -346.35 to -296.35 by 1.0 cm step	Probe calibration data: 1/31/14 Add 4 mm to *y* to align with Tosca. Calculate field box using Tosca grid, with *B* scaled to data at each *y*.	entry15.map, entry75.map, ... *x*: -1.4 to 14.6 by 1.0 *y*: -347.0 to -296.0 by 1.0

Table III. Field map alignment procedures. "X error" and "Y error" are data offsets relative to the Tosca calculations. Note that Configurations 1-4 are used to create the Main field box

Configuration	X error	X remedy	Y error	Y remedy
1	≈ −7 mm	Omit X=13.5 cm point and use Conf. 2	≈+8.5 mm	None: fringe region covered by Entry Box
2	−1.0 to 0.0 mm	Align $B_{max}/2$ point to Tosca at each Y value	Not significant: no trajectories near edge	None
3	≈ −3 mm	Omit X=13.5 cm point and use Conf. 4	≈+4 mm	None: fringe region covered by Exit box
4	−0.2 to +0.8 mm	Align $B_{max}/2$ point to Tosca at each Y value	≈ −10 mm	None: fringe region covered by Exit box
5	< −0.1 mm	None	< −0.6 mm	None
6	Not significant: no trajectories near edges	None	≈+4 mm (+1 mm after survey correction)	Use Tosca position in creating Entry box

Table IV. Field boxes for raytracing. The ".map" files are formatted for input to the SNAKE code (which is described in the document "Hall D Tagger Dipole Field Maps.") Because the default in SNAKE is to propagate the particle in the "y" direction, the internal coordinates of the Main and Focal ".map" boxes interchange the X and Y coordinates of the mapping system, and the coordinates of the Entry and Exit boxes are rotated by 90° relative to these. The X and Y coordinates in the ".txt" boxes are always in the mapping coordinate system.

Name	X limits and step [cm]	Y limits and step [cm]	Source	File names ("*NN*"=15,17 or 75)
MAIN	-14.5 to 51.5 by 1.0	-306.35 to 308.65 by 2.5	Conf. 1-4	`main`*`NN`*`.map` `main`*`NN`*`BXY.txt`
ENTRY	-1.4 to 14.6 by 1.0	-360.0 to -296.0 by 1.0	Conf. 6 and Tosca	`entry`*`NN`*`.map` `entry`*`NN`*`BXY.txt`
EXIT	0.5 to 70.5 by 1.0	2935.5 to 3606.5 by 1.0	Conf. 5 and Tosca	`exit`*`NN`*`.map` `exit`*`NN`*`BXY.txt`
FOCAL	46.6 to 70.6 by 2.0	-262.0 to 400.0 by 2.0	Tosca and Conf. 5	`focal`*`NN`*`.map` `focal`*`NN`*`BXY.txt`

Table V. Scale factors by which the map files must be multiplied to give 13.4° deflection of full-energy electrons at each map energy. The change due to probe recalibration is negligible, changing the electron energy calculations by less than 0.1 MeV anywhere.

Nominal field	Nominal energy	Before probe recalibration	After probe recalibration
1.7 T	13.6 GeV	1.001141	1.001166
1.5 T	12.0 GeV	1.000286	1.000302
0.75 T	6.0 GeV	1.000970	1.000983

Table VI. Consistency of the three field maps for energy reconstruction when scaled to the appropriate beam energy E_0. The maps at 1.7 T, 1.5 T and 0.75 T correspond to E_0 = 13.6, 12.0 and 6.0 GeV respectively.

E_0 [GeV]	Compare field maps	Difference in E/E_0 at given focal plane position	Error in E at given focal plane position when using 1.5 T map
13.6	1.7 T versus 1.5 T	-8×10^{-5} to $+2.5\times10^{-4}$	−1.1 to +3.4 MeV
6.0	0.75 T versus 1.5 T	-6×10^{-5} to $+1.3\times10^{-4}$	−0.4 to +0.8 MeV

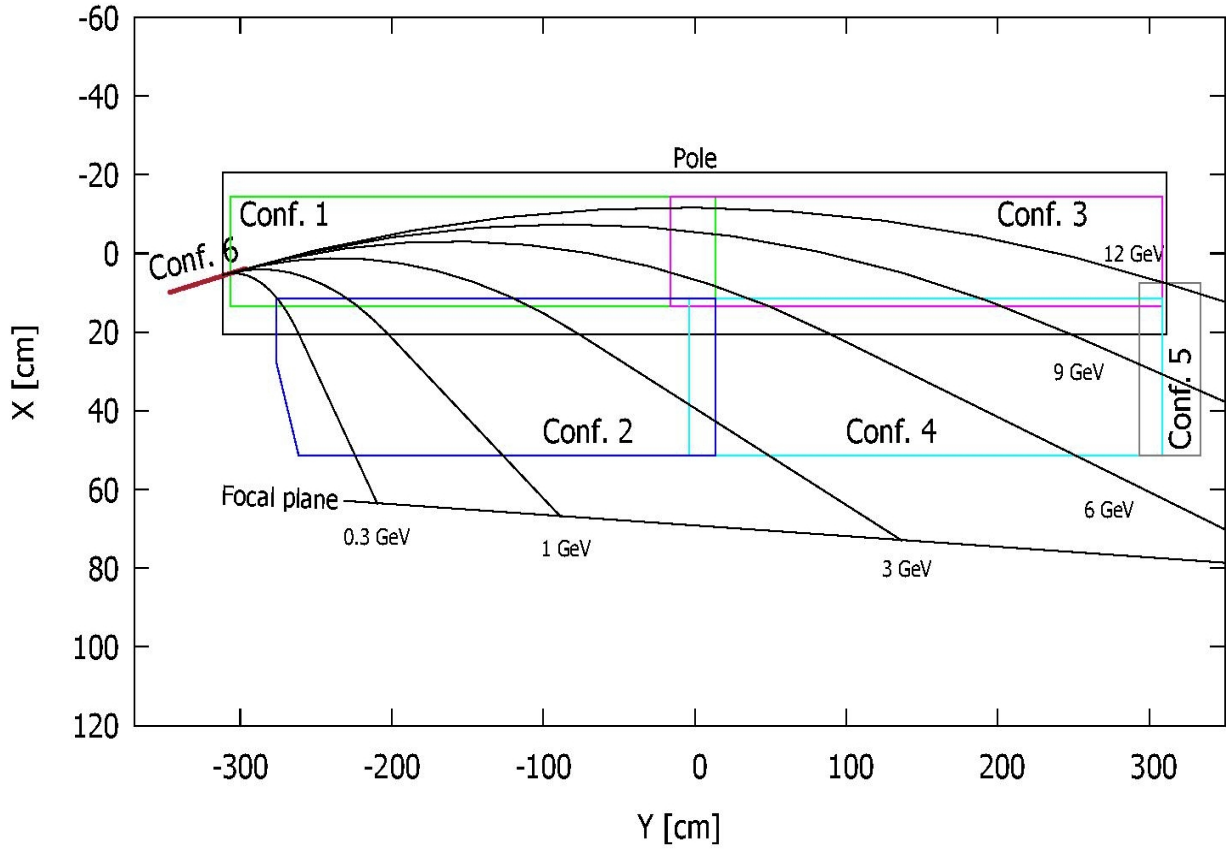

Figure 1 Boundaries of the six mapping configurations, together with selected electron trajectories. (Note large difference in X and Y scales.)

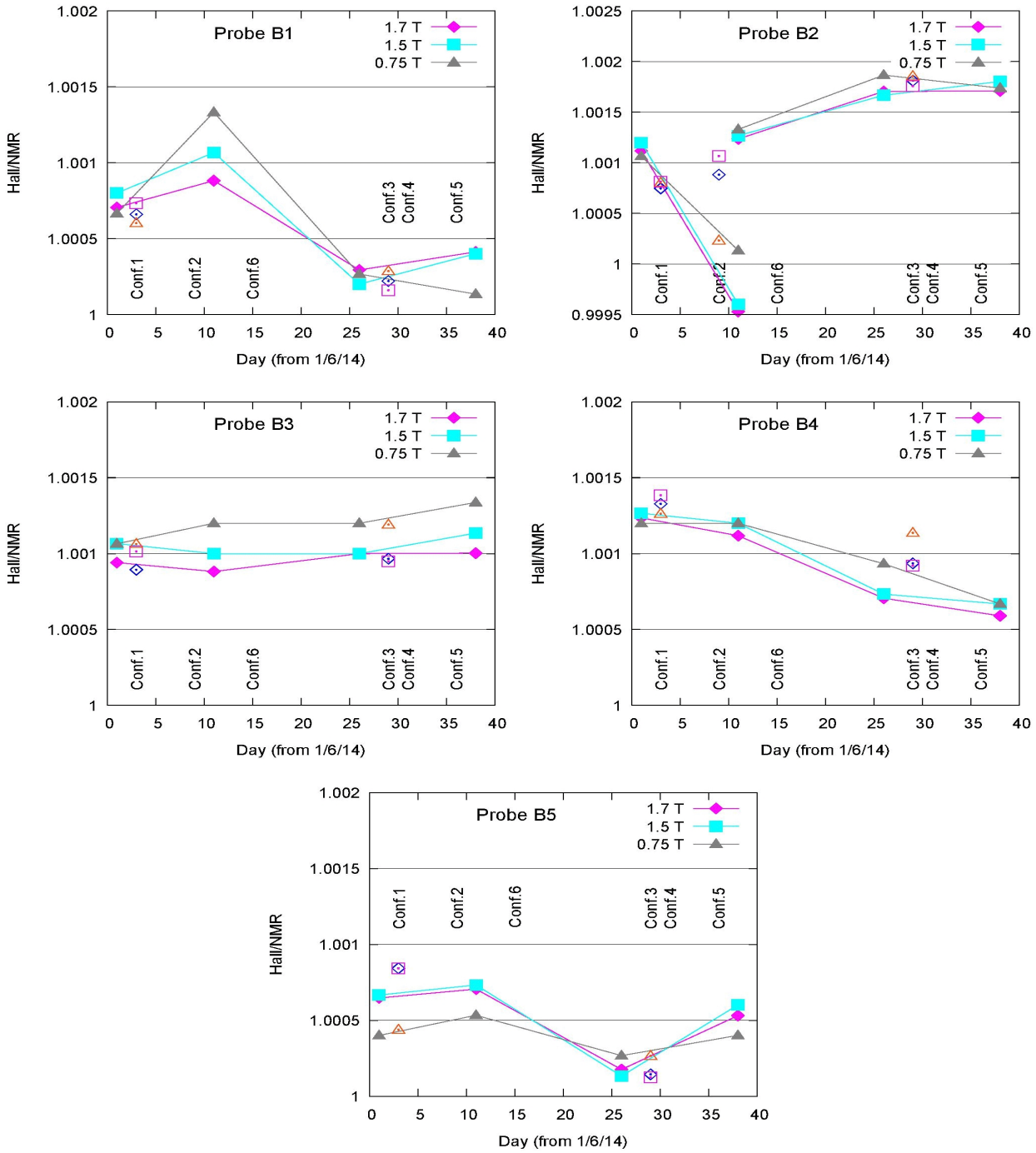

Figure 2 Probe calibration ratios (Hall probe/NMR) versus time. Probes B1-B5 are numbered in order of increasing X coordinate. The solid points, connected by lines, show the measured ratios. The open points of same shape show empirical values derived from data ratios in Configurations 1 and 3 (and, for Probe B2, Configuration 2). Probe B2 was replaced after Configuration 2.

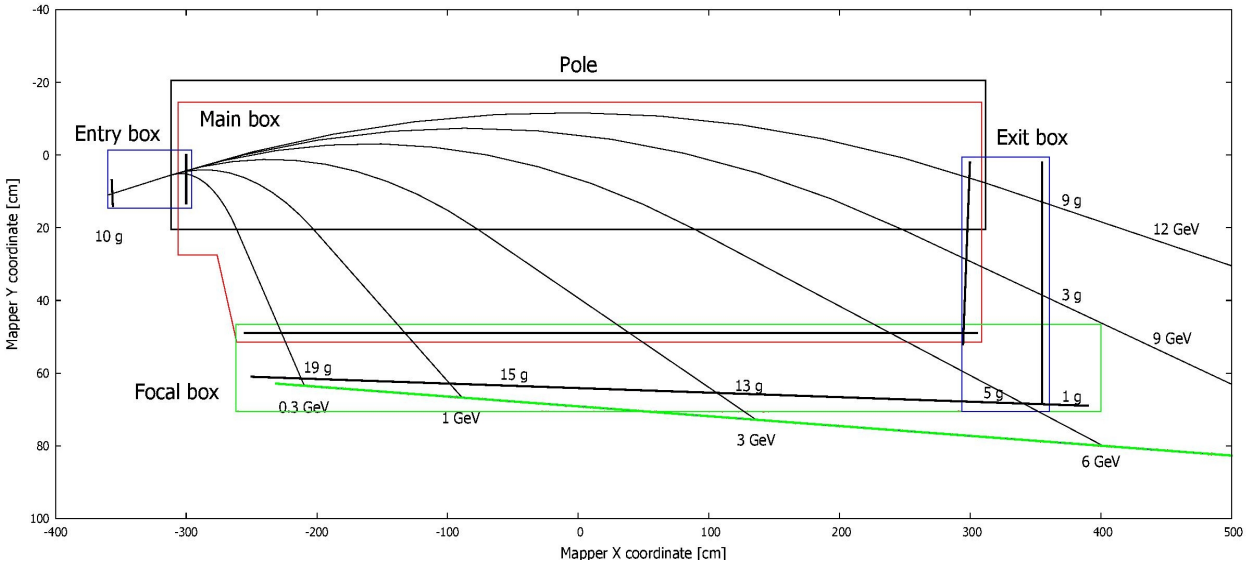

Figure 3. The four field boxes used in raytracing, together with the magnet pole, several electron trajectories, the focal plane and (thick black lines) the ”endplanes” at which a transition is made from one box to the next. After the final endplane in the Exit or Focal box the electron is propagated in a straight line. The numbers near the endplanes or box boundaries are the magnetic field values in gauss.

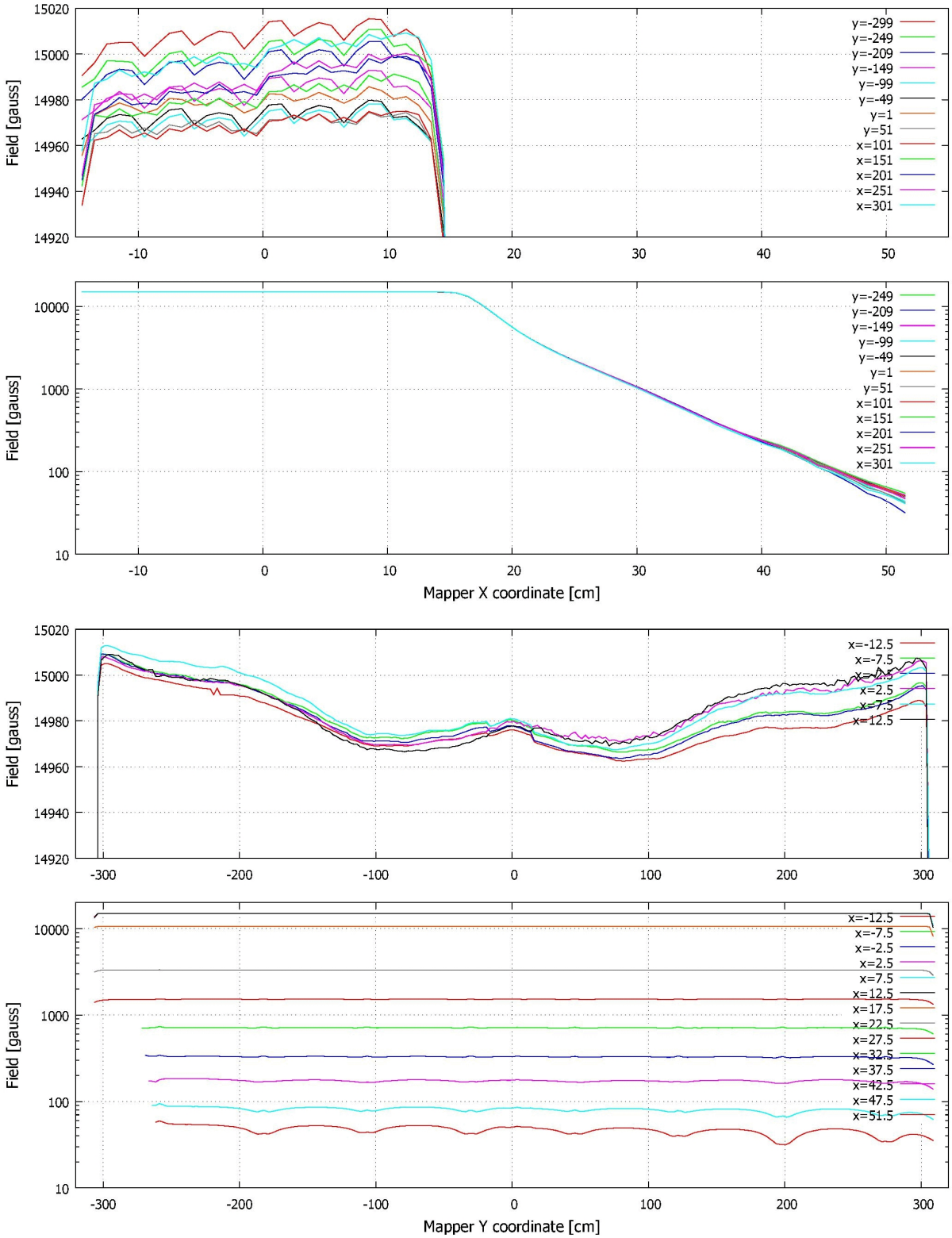

Figure 4. Magnetic field in Main field box before probe recalibration, plotted versus X (linear and semilog) and versus Y (linear and semilog.) The small oscillations versus X are due to the probe calibration factors, and were reduced by recalibration (next figure.) The small oscillations versus Y at low field are presumably due to focal plane hardware.

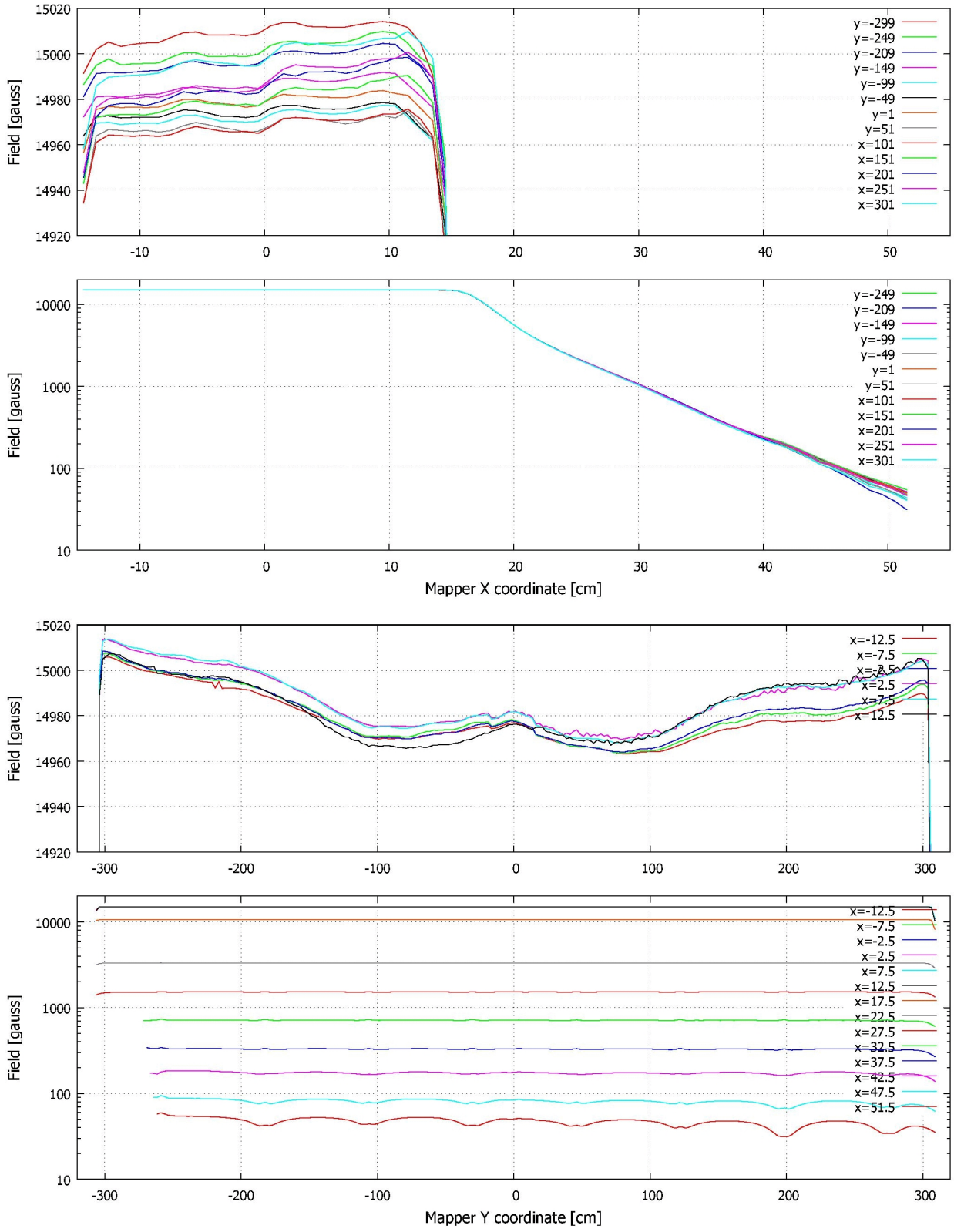

Figure 5. Same as Figure 4, but after probe recalibration.

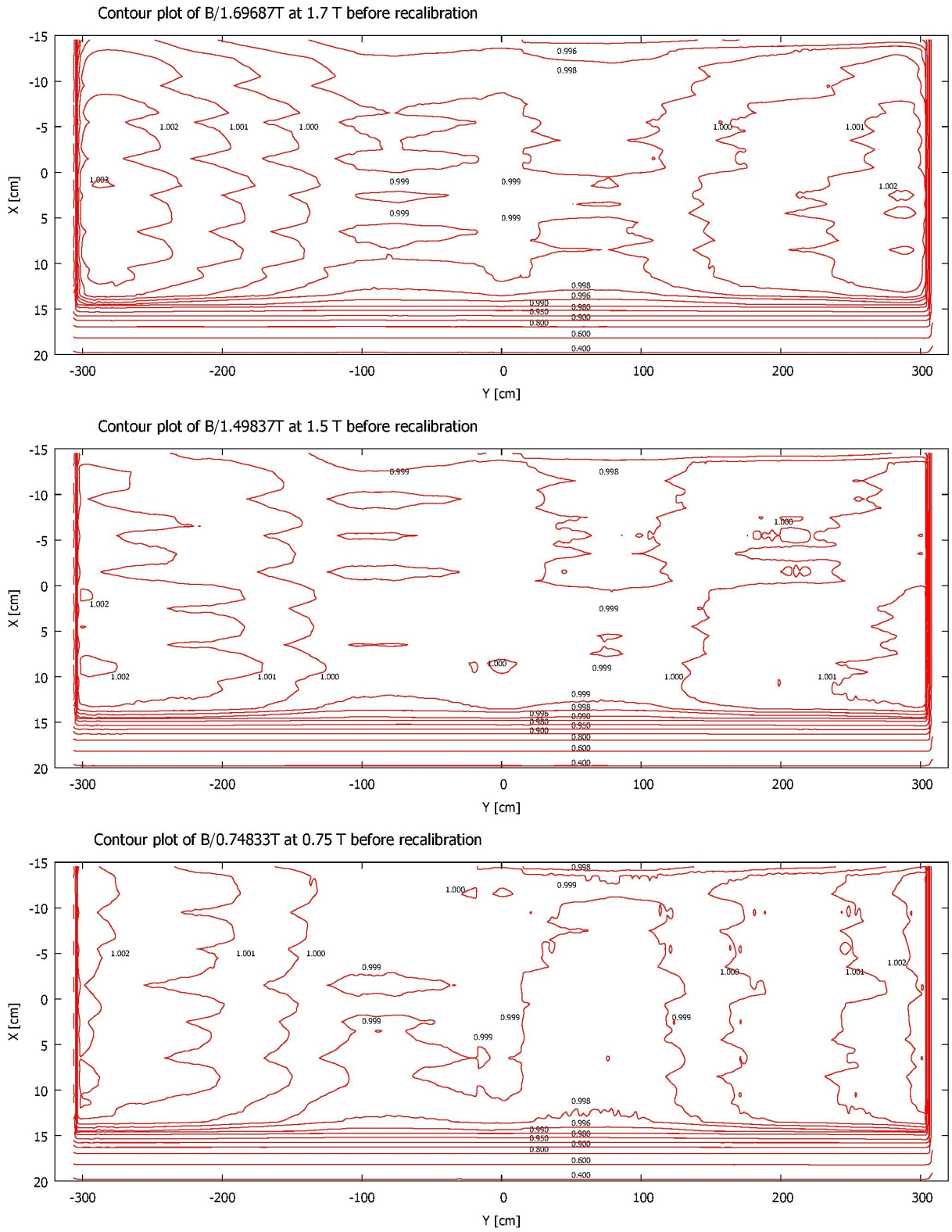

Figure 6. Contour plots of the magnetic field before recalibration, divided by the average field in the uniform region at each excitation. The periodicity versus X is due to small errors in the probe calibration factors.

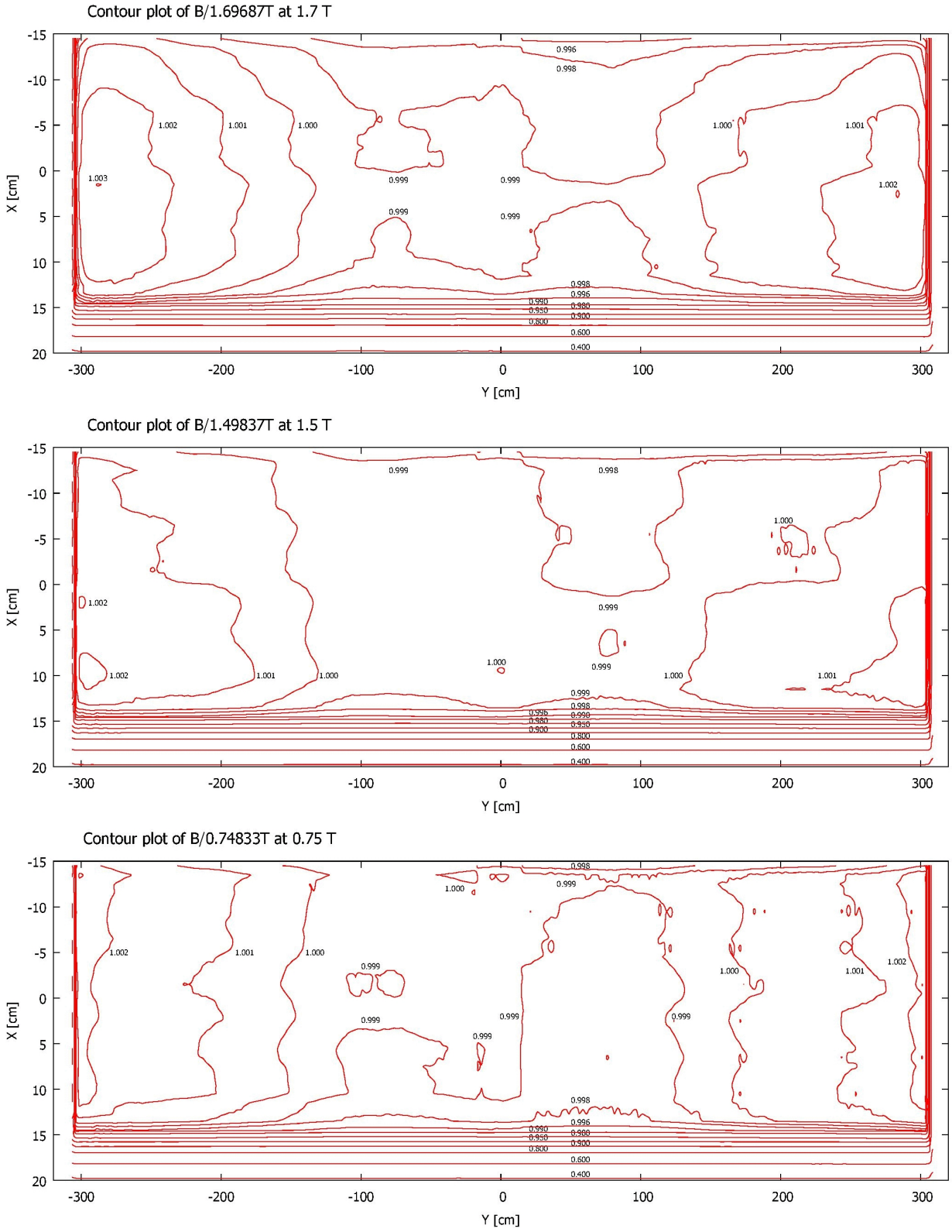

Figure 7. Same as Figure 6, but after probe recalibration.

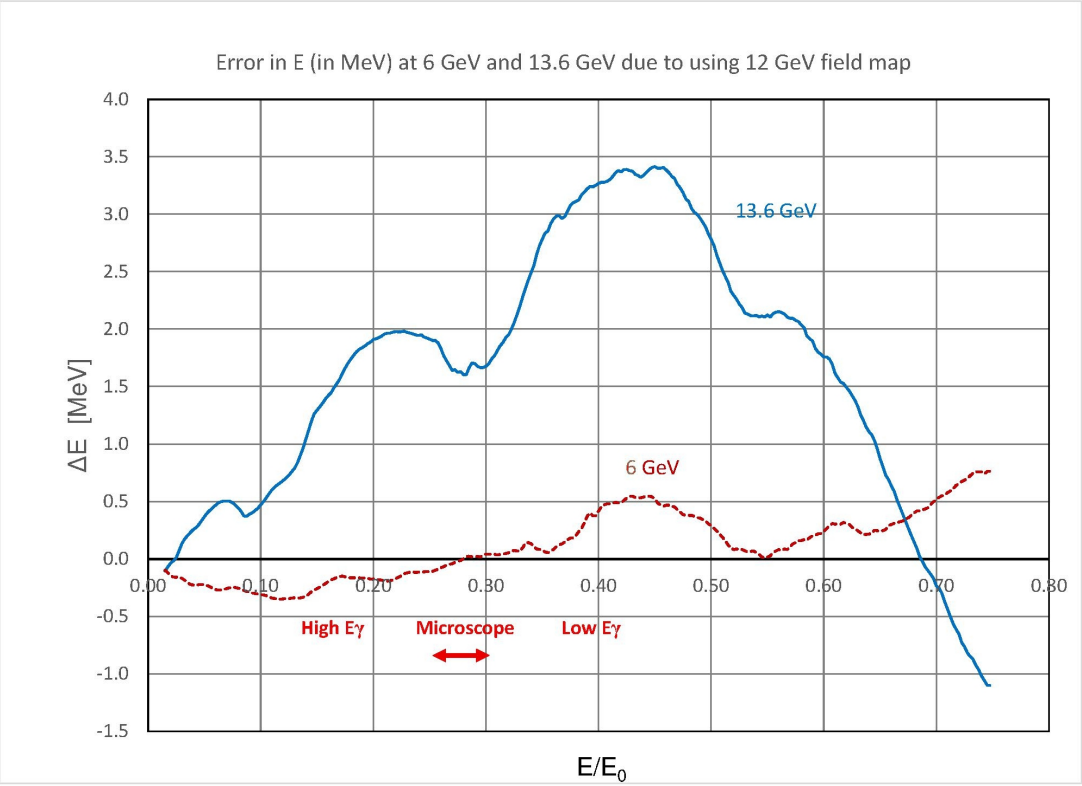

Figure 8. Error in E (in MeV) at E_0 = 6 GeV and 13.6 GeV due to using the scaled 12 GeV (1.5 T) field map for raytracing instead of the correct field map.